Proceedings of Meetings on Acoustics

Volume 23 http://acousticalsociety.org/

169th Meeting of the Acoustical Society of America

Pittsburgh, Pennsylvania
18-22 May 2015

Underwater Acoustics: Paper 1pUW12

Second-order statistics of the instantaneous mutual information in time-varying underwater particle velocity channels

Chen Chen and **Shuangquan Wang**
Samsung Mobile Solution Lab, San Diego, CA 92121, USA; cc224@njit.edu; sw27@njit.edu

Ali Abdi
Center for Wireless Communications and Signal Processing Research, New Jersey Institute of Technology, Newark, NJ 07102, USA; ali.abdi@njit.edu

Instantaneous mutual information (IMI) is the amount of information that a time-varying channel can convey for the given time instant. In this paper, second-order statistics of IMI are studied in time-varying underwater particle velocity channels. First, the autocorrelation function, correlation coefficient, level crossing rate and average outage duration of IMI are provided in a time-varying fading channel. Exact expressions are given in terms of the summation of special functions, which facilitate numerical calculations. Then accurate approximations for the autocorrelation function and correlation coefficient are presented for low and high signal-to-noise ratios (SNRs). Moreover, analytical and numerical results are provided for the correlation and level-crossing characteristics of IMI in underwater particle velocity channels. The results shed light on the dynamic behavior of mutual information in underwater particle velocity channels.

Published by the Acoustical Society of America

 [DOI: 10.1121/2.0000081]
Received 30 August 2015; Published 09 September 2015

I. INTRODUCTION

The underwater environment is a dynamic and time-varying channel. Communication and signal processing in a time-varying channel need the knowledge of the temporal characteristics of the channel. Space-time correlation function of the underwater pressure channel has been studied in [1]-[3]. Temporal correlation of underwater particle velocity channels is studied recently in [4], to calculate the Doppler spread of such channels in multipath underwater environments. Particle velocity channels have recently been considered for underwater communication [5]-[7]. For recent developments on temporal correlation, one can refer to [8].

Another quantity of interest in modeling signal transmission in time-varying channels is the instantaneous mutual information (IMI). It specifies the amount of information in any given time instant that can be transmitted through a channel from a transmitter to a receiver. In a time-varying channel, IMI changes with time. If the fluctuating IMI stays below a certain data rate threshold for a specific time period, it necessitates a low transmission rate over that period, otherwise, considerable signaling errors will occur. Quantities such as outage probabilities do not show the temporal dynamic behavior of IMI in a time-varying channel. Outage probability, for example, gives the probability of IMI to be smaller than a particular data rate [9]. However, it does not show for how long the IMI stays below that data rate. This inspired us to study the time-varying behavior of IMI and its second order statistics.

As an application of IMI, we note that IMI can be fedback to the rate scheduler in multi-user communication systems to increase the system throughput [10]. Hochwald et al. [10] considered no delay between the decision and transmission. However, typically there is a propagation delay in practical communication systems. This delay is especially large in underwater channels [11]. So, one can naturally ask how much the multiuser diversity gain degrades if the channel is time-varying and there is a delay between the scheduling decision and signal transmission. To answer this question, the second-order statistics, especially the temporal correlation coefficient of IMI is needed. For example, we have the full multiuser diversity gain if IMI is fully correlated and no multiuser diversity gain if IMI samples are uncorrelated [12] [13]. Upon taking into account the propagation delay, one can develop a better rate scheduler, by exploiting the second-order statistics of IMI.

There are a limited number of papers which have studied IMI in radio frequency channels [14]-[17]. To the best of our knowledge, the problem has not been addressed in underwater channels. In this paper, we focus on important second-order statistics such as the autocorrelation, correlation coefficient, level crossing rate (LCR) and average outage duration (AOD) of IMI for time-varying particle velocity channels in shallow waters. Closed-form expressions and simple approximations are provided for the autocorrelation function (ACF), correlation coefficient, LCR and AOD of particle velocity IMI. The results show that the correlation coefficient of IMI can be closely approximated by the squared amplitude of the normalized correlation coefficient of the channel, for all SNRs. Numerical results are also provided to verify the derived closed-form expressions.

The rest of the paper is organized as follows. In Sec. II the IMI random process is defined and then the ACF, correlation coefficient, LCR and AOD of IMI are derived. Sec. III is devoted

to studying the ACF, correlation coefficient, LCR and AOD of IMI in underwater particle velocity channels. Concluding remarks are given in Sec. IV.

II. SECOND ORDER STATISTICS OF THE INSTANTANEOUS MUTUAL INFORMATION

In this paper, a discrete-time fading channel model is considered, represented by $\{h(lT_s)\}_{l=1}^{L}$, where T_s is the symbol duration and L is the number of samples. In what follows, we drop T_s to simplify the notation.

In a Rayleigh fading channel, the channel coefficient $h(l)$, $l \in [1, L]$, is a zero-mean complex Gaussian random process. In the l^{th} interval, $h(l)$ can be represented by [18]

$$h(l) = h_I(l) + jh_Q(l), \tag{1}$$

where $h_I(l)$ and $h_Q(l)$ are the in-phase and quadrature components of $h(l)$, respectively and $j = \sqrt{-1}$. Note that $h_I(l)$ and $h_Q(l)$ are independent and identically-distributed real Gaussian random variables at any time index l. The average channel power Ω is defined as $\Omega = E[|h(l)|^2]$, $\forall l$, where $E[\cdot]$ is the mathematical expectation.

At any given time index l, $\log_2(1+\eta|h(l)|^2)$ is a random variable as it depends on the fading channel $h(l)$ [19], where $\log_2$ is the base-2 logarithm and η is the average SNR at the receiver. Therefore,

$$\mathscr{I}_l = \log_2(1+\eta|h(l)|^2), \quad l = 1, 2, \cdots, \tag{2}$$

is the discrete-time IMI random process.

A. Autocorrelation Function and Correlation Coefficient

The ACF of IMI is defined by [17] [20]

$$\begin{aligned} r_{\mathscr{I}}(i) &= E[\mathscr{I}_l \mathscr{I}_{l-i}], \\ &= (\log_2 e)^2 E[\ln(1+\eta X_0)\ln(1+\eta X_i)], \end{aligned} \tag{3}$$

where $X_k = |h(l-k)|^2$, $\forall k$, and ln is the natural logarithm. The joint probability density function (PDF) of X_0 and X_i is given by [19] [21]

$$p(x_0, x_i) = \frac{\lambda_i}{\Omega^2} e^{-\frac{\lambda_i(x_0+x_i)}{\Omega}} I_0\left(\frac{2\lambda_i\varsigma_i\sqrt{x_0 x_i}}{\Omega}\right), \tag{4}$$

where $\lambda_i = \frac{1}{1-\varsigma_i^2}$, $\varsigma_i = \left|\frac{\rho_h(i)}{\Omega}\right| < 1$, $i \neq 0$, $\rho_h(i) = E[h(l)h^*(l-i)]$ is the channel autocorrelation with * as complex conjugate, and $I_0(.)$ is the zero order modified Bessel function. As shown in [20], the normalized ACF of IMI is given by

$$\tilde{r}_{\mathscr{I}}(i) = \frac{r_{\mathscr{I}}(i)}{E[\mathscr{I}_l^2]} = \frac{\lambda_i \sum_{k=0}^{\infty} \frac{(\lambda_i \varsigma_i)^{2k}}{(k!)^2} \left[\int_0^{\infty} x^k e^{-\lambda_i x} \ln(1+\eta\Omega x) dx\right]^2}{2e^{\frac{1}{\eta\Omega}} G_{2,3}^{3,0}\left(\frac{1}{\eta\Omega}\middle|_{0,0,0}^{1,1}\right)} = \frac{\frac{1}{\lambda_i}\sum_{k=0}^{\infty}\left[\frac{\varsigma_i^k}{k!} G_{2,3}^{3,1}\left(\frac{\lambda_i}{\eta\Omega}\middle|_{0,0,k+1}^{0,1}\right)\right]^2}{2e^{\frac{1}{\eta\Omega}} G_{2,3}^{3,0}\left(\frac{1}{\eta\Omega}\middle|_{0,0,0}^{1,1}\right)}. \quad (5)$$

Here G is Meijer's G function [20].

Similarly, after some algebraic manipulations, the correlation coefficient of IMI is obtained as

$$\begin{aligned} \rho_{\mathscr{I}}(i) &= \frac{r_{\mathscr{I}}(i) - \{E[\mathscr{I}_l]\}^2}{E[\mathscr{I}_l^2] - \{E[\mathscr{I}_l]\}^2}, \\ &= \frac{\frac{1}{\lambda_i}\sum_{k=0}^{\infty}\left[\frac{\varsigma_i^k}{k!} G_{2,3}^{3,1}\left(\frac{\lambda_i}{\eta\Omega}\middle|_{0,0,k+1}^{0,1}\right)\right]^2 - e^{\frac{2}{\eta\Omega}}\Gamma^2(0,\frac{1}{\eta\Omega})}{2e^{\frac{1}{\eta\Omega}} G_{2,3}^{3,0}\left(\frac{1}{\eta\Omega}\middle|_{0,0,0}^{1,1}\right) - e^{\frac{2}{\eta\Omega}}\Gamma^2(0,\frac{1}{\eta\Omega})}, \end{aligned} \quad (6)$$

where $\Gamma(a,z) = \int_z^{\infty} t^{a-1}e^{-t}dt$ is the upper incomplete gamma function [22].

Upon using the integral $\Xi(k,\eta,\lambda_i) = \int_0^{\infty} x^k e^{-\lambda_i x} \ln(1+\eta\Omega x) dx$, $k \geq 0$, which can be approximated by

$$\Xi(k,\eta,\lambda_i) = \begin{cases} \int_0^{\infty} \eta\Omega x^{k+1} e^{-\lambda_i x} dx, & \eta\Omega \to 0, \\ \int_0^{\infty} x^k e^{-\lambda_i x} \ln(\eta\Omega x) dx, & \eta\Omega \to \infty, \end{cases} \quad (7)$$

asymptotic closed-form expressions for $r_{\mathscr{I}}(i)$ in low and high-SNR regimes are derived, respectively [20]. In low-SNR regime we have

$$\tilde{r}_{\mathscr{I}}(i) \approx \frac{1+\varsigma_i^2}{2}, \quad (8)$$

and

$$\rho_{\mathscr{I}}(i) \approx \frac{r_{\mathscr{I}}(i) - \{(\log_2 e)E[\eta X_0]\}^2}{E[\mathscr{I}_l^2] - \{(\log_2 e)E[\eta X_0]\}^2} = \frac{\eta^2\Omega^2(1+\varsigma_i^2) - \eta^2\Omega^2}{2\eta^2\Omega^2 - \eta^2\Omega^2} = \varsigma_i^2. \tag{9}$$

In high-SNR regime, expression for the normalized ACF is given by [20]

$$\tilde{r}_{\mathscr{I}}(i) \approx \frac{\mathrm{Li}_2(\varsigma_i^2) + \ln^2\dfrac{\eta\Omega}{\gamma}}{\dfrac{\pi^2}{6} + \ln^2\dfrac{\eta\Omega}{\gamma}}, \tag{10}$$

where $\mathrm{Li}_2(x)$ is the logarithm function, defined as $\mathrm{Li}_2(x) = \sum_{k=1}^{\infty}\frac{x^k}{k^2}$, $|x| \le 1$. Note that $\mathrm{Li}_2(1) = \frac{\pi^2}{6}$ and $\gamma = 1.781072\cdots$ is the Euler-Mascheroni constant [22]. The correlation coefficient can be verified to be

$$\rho_{\mathscr{I}}(i) \approx \frac{6\mathrm{Li}_2(\varsigma_i^2)}{\pi^2}. \tag{11}$$

B. Level Crossing Rate and Average Outage Duration of Instantaneous Mutual Information

Level Crossing Rate: Define the binary sequence $\{Z_l\}_{l=1}^{L}$, based on the IMI sequence $\{\mathscr{I}_l\}_{l=1}^{L}$, such that [20] [23]

$$Z_l = \begin{cases} 1, & \text{if } \mathscr{I}_l \ge \mathscr{I}_{\mathrm{th}}, \\ 0, & \text{if } \mathscr{I}_l < \mathscr{I}_{\mathrm{th}}, \end{cases} \tag{12}$$

where $\mathscr{I}_{\mathrm{th}}$ is a fixed threshold. Within the time interval $T_s \le t \le LT_s$, the number of crossings of $\{\mathscr{I}_l\}_{l=1}^{L}$ with $\mathscr{I}_{\mathrm{th}}$, denoted by $D_{\mathscr{I}}(\mathscr{I}_{\mathrm{th}})$, is defined as [20] [23]

$$D_{\mathscr{I}}(\mathscr{I}_{\mathrm{th}}) = \sum_{l=2}^{L}(Z_l - Z_{l-1})^2, \tag{13}$$

which includes both up and down-crossings. After some mathematical manipulations, LCR of IMI at the level $\mathscr{I}_{\mathrm{th}}$ can be shown to be [20]

$$\frac{E[D_{\mathscr{I}}(\mathscr{I}_{\mathrm{th}})]}{(L-1)T_s} = 2N_{\mathscr{I}}(\mathscr{I}_{\mathrm{th}}) = \frac{2e^{-\frac{2^{\mathscr{I}_{\mathrm{th}}}-1}{\eta\Omega}}}{T_s} - \frac{2-2\varsigma_1^2}{T_s}\sum_{k=0}^{\infty}\left[\frac{\varsigma_1^k}{k!}\Gamma\left(k+1, \frac{2^{\mathscr{I}_{\mathrm{th}}}-1}{\eta\Omega(1-\varsigma_1^2)}\right)\right]^2. \tag{14}$$

Average Outage Duration: The AOD of IMI, normalized by T_s, is given by [20]

$$\frac{\tilde{t}_{\mathscr{I}}(\mathscr{I}_{\text{th}})}{T_s}=\frac{F_{\mathscr{I}}(\mathscr{I}_{\text{th}})}{T_s N_{\mathscr{I}}(\mathscr{I}_{\text{th}})}=\frac{1-e^{-\frac{2^{\mathscr{I}_{\text{th}}}-1}{\eta\Omega}}}{e^{-\frac{2^{\mathscr{I}_{\text{th}}}-1}{\eta\Omega}}-(1-\varsigma_1^2)\sum_{k=0}^{\infty}\left[\frac{\varsigma_1^k}{k!}\Gamma(k+1,\frac{2^{\mathscr{I}_{\text{th}}}-1}{\eta\Omega(1-\varsigma_1^2)})\right]^2}, \tag{15}$$

where

$$F_{\mathscr{I}}(\mathscr{I}_{\text{th}})=\Pr\{X_0\le\frac{2^{\mathscr{I}_{\text{th}}}-1}{\eta}\}=\int_0^{\frac{2^{\mathscr{I}_{\text{th}}}-1}{\eta}}\frac{1}{\Omega}e^{-\frac{x_0}{\Omega}}dx_0=1-e^{-\frac{2^{\mathscr{I}_{\text{th}}}-1}{\eta\Omega}} \tag{16}$$

is the cumulative distribution function (CDF) of IMI, obtained based on the relationship between $\mathscr{I}_l$ and $X_0=|h(l)|^2$ in (2), and using the PDF of X_0.

III. NUMERICAL RESULTS FOR UNDERWATER PARTICLE VELOCITY CHANNELS

As demonstrated in [24] using collected experimental data, underwater particle velocity channels follow the Rayleigh distribution. Therefore, in this section we can use the analytical results presented in the previous section, to study the dynamics of instantaneous mutual information in underwater particle velocity channels.

A. Equations for Underwater Particle Velocity Second-Order Statistics

In a typical shallow water shown in Fig. 1, the rays impinging the receiver come from the sea bottom and the sea surface. Suppose γ_b and γ_s are the angle-of-arrivals (AoAs) of rays coming from the bottom and the surface, respectively, observed at the vector sensor receiver labeled as *Rx* in Fig. 1, φ_0 specifies the direction of the mobile vector sensor receiver with respect to the horizon, and $f_d=(Rx\,\text{speed})/\lambda$ is the maximum Doppler frequency, where λ is the wavelength. Let the *y*-velocity and *z*-velocity channels, symbolically shown in Fig. 1 by thick arrows, be the gradients of the acoustic pressure measured by the vector sensor receiver in *y* and *z* directions, respectively [5]. The temporal correlation functions for the *y*-velocity and *z*-velocity channels are given by [4]

$$\varsigma_y(i)=\Lambda_b E_{\gamma_b}[\cos^2(\gamma_b)e^{j2\pi iT_s f_d\cos(\gamma_b-\varphi_0)}]+(1-\Lambda_b)E_{\gamma_s}[\cos^2(\gamma_s)e^{j2\pi iT_s f_d\cos(\gamma_s-\varphi_0)}], \tag{17}$$

$$\varsigma_z(i) = \Lambda_b E_{\gamma_b}[\sin^2(\gamma_b) e^{j2\pi i T_s f_d \cos(\gamma_b - \varphi_0)}] + (1-\Lambda_b) E_{\gamma_s}[\sin^2(\gamma_s) e^{j2\pi i T_s f_d \cos(\gamma_s - \varphi_0)}], \quad (18)$$

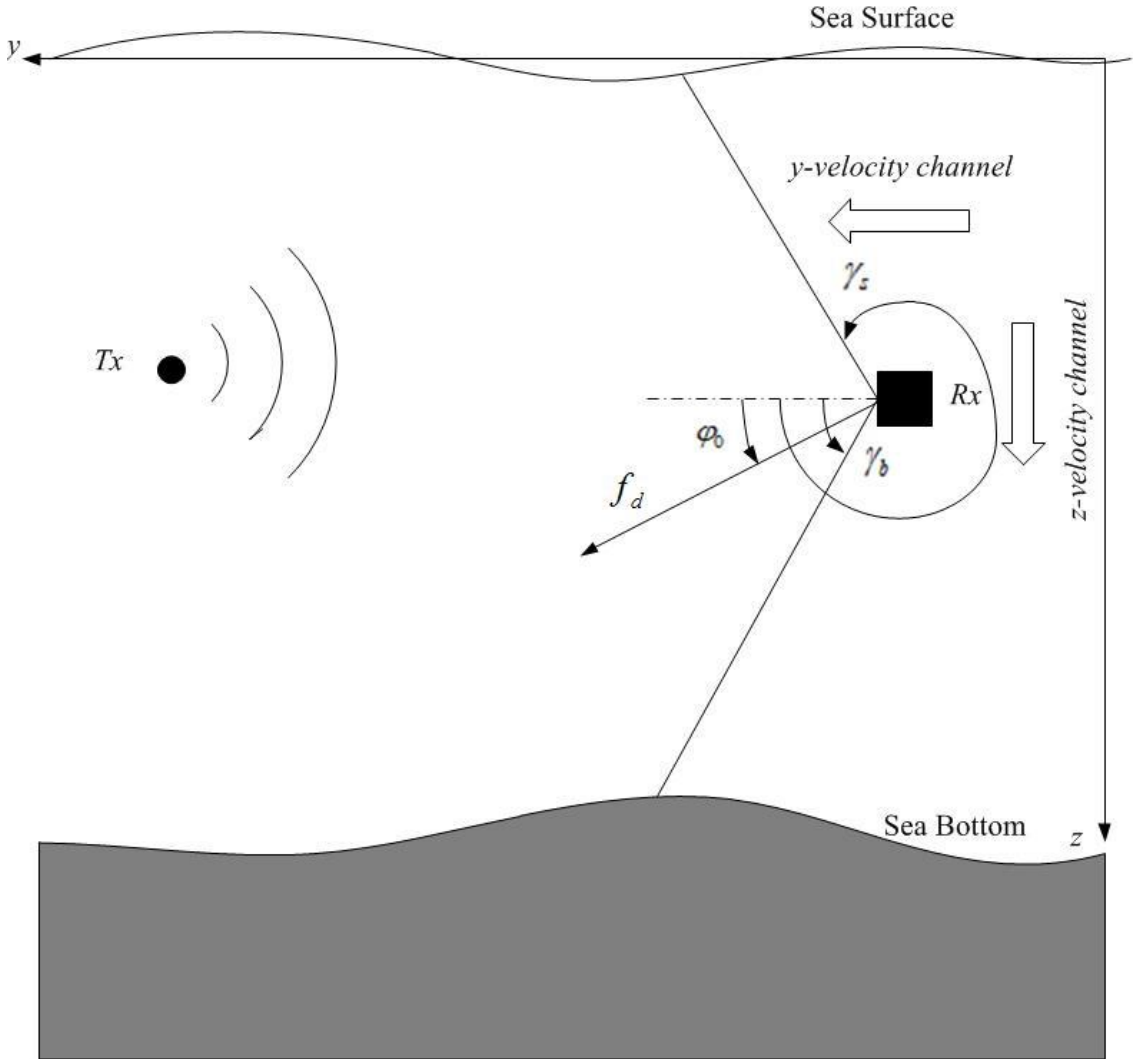

FIGURE 1. A Mobile Vector Sensor Communication Receiver in Shallow Water.

where Λ_b is the proportion of power received from the sea bottom. Consider that the AoA of rays from the sea bottom follows a Gaussian distribution with mean and variance (μ_b, σ_b^2), whereas the AoA of rays from the sea surface forms a Gaussian distribution with parameters (μ_s, σ_s^2) [25]. For small angle spreads in shallow waters [25], (17) and (18) can be shown to be [4]

$$
\begin{aligned}
\varsigma_y(i) \approx{}& \Lambda_b e^{j2\pi i T_s f_d \cos(\mu_b-\varphi_0)-2\sigma_b^2\pi^2 f_d^2 i^2 T_s^2 \sin^2(\mu_b-\varphi_0)} \\
&\times[\cos^2(\mu_b)-\sigma_b^2\sin^2(\mu_b)-4\pi i T_s f_d \sigma_b^2\cos(\mu_b)\sin(\mu_b)\sin(\mu_b-\varphi_0) \\
&+4(\pi i T_s f_d \sigma_b^2 \sin(\mu_b)\sin(\mu_b-\varphi_0))^2] \\
&+(1-\Lambda_b)e^{j2\pi i T_s f_d \cos(\mu_s-\varphi_0)-2\sigma_s^2\pi^2 f_d^2 i^2 T_s^2 \sin^2(\mu_s-\varphi_0)} \\
&\times[\cos^2(\mu_s)-\sigma_s^2\sin^2(\mu_s)-4\pi i T_s f_d \sigma_s^2\cos(\mu_s)\sin(\mu_s)\sin(\mu_s-\varphi_0) \\
&+4(\pi i T_s f_d \sigma_s^2 \sin(\mu_s)\sin(\mu_s-\varphi_0))^2],
\end{aligned}
\tag{19}
$$

$$
\begin{aligned}
\varsigma_z(i) \approx{}& \Lambda_b e^{j2\pi i T_s f_d \cos(\mu_b-\varphi_0)-2\sigma_b^2\pi^2 f_d^2 i^2 T_s^2 \sin^2(\mu_b-\varphi_0)} \\
&\times[\sin^2(\mu_b)-\sigma_b^2\cos^2(\mu_b)+4\pi i T_s f_d \sigma_b^2\cos(\mu_b)\sin(\mu_b)\sin(\mu_b-\varphi_0) \\
&+4(\pi i T_s f_d \sigma_b^2 \cos(\mu_b)\sin(\mu_b-\varphi_0))^2] \\
&+(1-\Lambda_b)e^{j2\pi i T_s f_d \cos(\mu_s-\varphi_0)-2\sigma_s^2\pi^2 f_d^2 i^2 T_s^2 \sin^2(\mu_s-\varphi_0)} \\
&\times[\sin^2(\mu_s)-\sigma_s^2\cos^2(\mu_s)+4\pi i T_s f_d \sigma_s^2\cos(\mu_s)\sin(\mu_s)\sin(\mu_s-\varphi_0) \\
&+4(\pi i T_s f_d \sigma_s^2 \cos(\mu_s)\sin(\mu_s-\varphi_0))^2].
\end{aligned}
\tag{20}
$$

By replacing ς_i in (6) with the correlation expressions $\varsigma_y(i)$ and $\varsigma_z(i)$ given in (19) and (20), respectively, IMI correlation coefficient for any SNR in *y*-velocity and *z*-velocity channels can be computed. For low and high SNRs, equations (9) and (11) provide simpler alternatives, respectively. To obtain LCR and AOD of IMI, one can use (14) and (15), respectively.

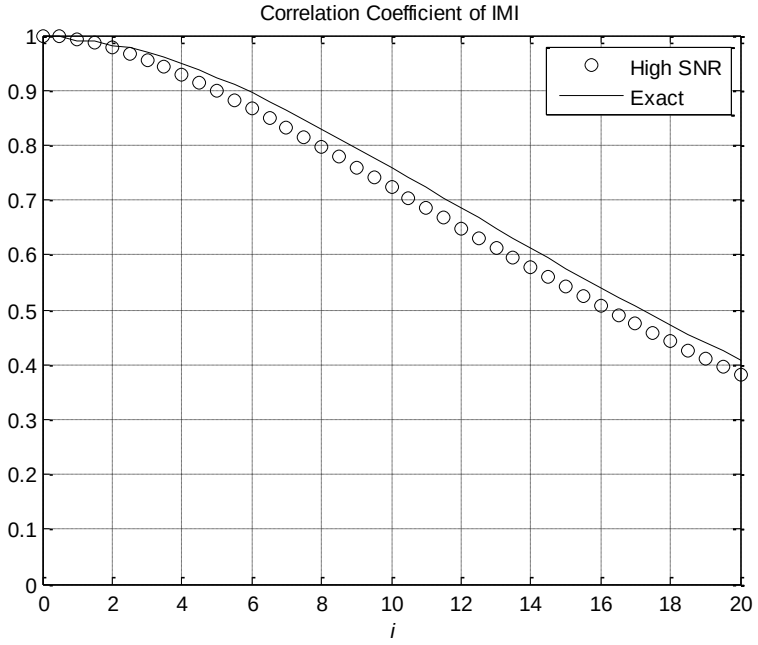

Figure 2. Correlation coefficient of IMI in the *z* velocity channel ($\eta = 20\,\mathrm{dB}$).

B. Numerical Results

To show how the derived results can be used and what the physical implications are, here we provide some numerical examples for the z channel. For $(\mu_b, \sigma_b) = (\pi/36, \pi/90)$, $(\mu_s, \sigma_s) = (29\pi/15, \pi/120)$, $\Lambda_b = 0.4$, $f_d = 10\,\text{Hz}$, $\varphi_0 = 0$ and $T_s = 0.1\,\text{sec.}$, the correlation coefficient, LCR and AOD of IMI are shown in Figs. 2-4, respectively. In Fig. 2 we observe that for the high SNR of $\eta = 20\,\text{dB}$, the simpler high SNR IMI correlation formula in (11) agrees well with the exact expression. According to Fig. 3, the level crossing of IMI has a peak whose location shifts to the right, as SNR increases. For example, for $\eta = 5$ and $10\,\text{dB}$, IMI level crossing is maximum at 1.3 and 2.6 bps/Hz, respectively. This agrees with the intuition that as SNR increases, IMI in the time-varying channel fluctuates around a higher data rate. Fig. 4 conveys another interesting message. Suppose we are interested in the threshold spectral efficiency of 4 bps/Hz in a time-varying underwater channel. According to Fig. 4 and for the SNR of 5 dB, IMI stays below this threshold for 230 sec. on average. The outage duration with respect to the same threshold but at the higher SNR of 10 dB becomes 12 sec. This is in line with the intuition that by increasing SNR, the IMI outage duration should decrease.

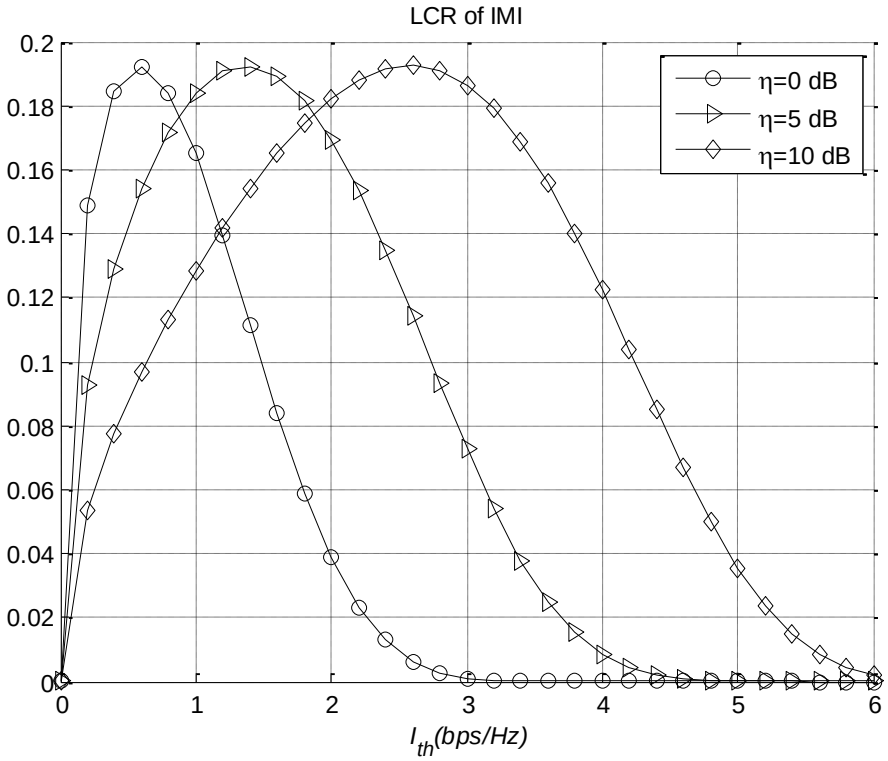

Figure 3. Level crossing rate of IMI in the z velocity channel.

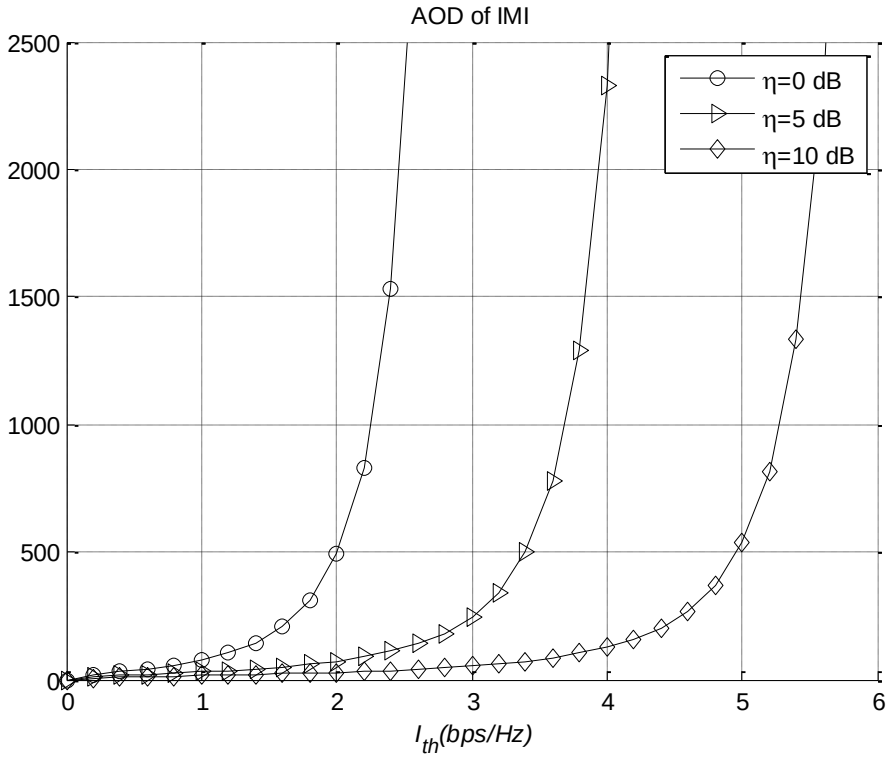

Figure 4. Average outrage duration of IMI in the z velocity channel, normalized by the sampling period T_s.

IV. CONCLUSIONS

In this paper, the dynamical characteristics of the mutual information in time-varying underwater particle velocity channels are studied. More specifically, closed-form expressions are derived for the level crossing rate and average outage duration of the instantaneous mutual information (IMI), as well as its autocorrelation function and correlation coefficient. The derived results show that IMI's temporal fluctuations depend on the Doppler spread, signal-to-noise ratio, and the angle-of-arrival statistics. For example, as the angle spread at the receiver increases, IMI samples are shown to become less correlated in time, which means faster fluctuation of IMI. This agrees with the increased level crossing rate of IMI, another result derived in this paper. Quantification of the average outage duration of IMI is another outcome of this work. Overall, the results are useful for analysis and design of systems in time-varying underwater particle velocity channels.

ACKNOWLEDGEMENTS

This work is supported in part by the National Science Foundation (NSF), Grant CCF-0830190.

REFERENCES

[1] A. G. Zajic, "Statistical modeling of MIMO mobile-to-mobile underwater channels," IEEE Trans. Veh. Technol. **60**, 1337-1351 (2011).

[2] B. Blankenagal, A. G. Zajic, "Simulation model for wideband mobile-to-mobile underwater fading channels," in *Proc. IEEE Veh. Technol. Conf.* (Dresden, 2013), pp. 1-5.

[3] B. Blankenagal, A. G. Zajic, "Envelope level crossing rate in mobile-to-mobile underwater fading channel," in *Proc. IEEE Int. Conf.* on *Commun.* (Budapest, 2013), pp. 5057-5061.

[4] H. Guo, A. Abdi, A. Song and M. Badiey, "Characterization of delay and Doppler spreads of underwater particle velocity channels using zero crossing rates," in *Proc. Conf. Inform. Sci. Syst.* (Princeton, NJ, 2010), pp. 1-6.

[5] A. Abdi and H. Guo, "A new compact multichannel receiver for underwater wireless communication networks," IEEE Trans. Wireless Commun. **8**, 3326-3329 (2009).

[6] C. Chen and A. Abdi, "Signal transmission using underwater acoustic vector transducers," IEEE Trans. Signal Processing **61**, 3683-3698 (2013).

[7] C. Chen and A. Abdi, "Utilization of underwater particle velocity channels for data transmission: Signals, channels and system performance," in *Proc. IEEE Intel. Conf.* on *Commun*. (Ottawa, ON, 2012), pp. 3816-3820.

[8] P. Karadimas and J. Zhang, "A generalized analysis of three-dimensional anisotropic scattering in mobile wireless channels-part II: Second-order statistical characterization," in *Proc. IEEE Veh. Technol. Conf.* (Quebec City, QC, 2012), pp.1-5.

[9] D. Tse and P. Viswanath, *Fundamentals of Wireless Communication* (Cambridge, UK: Cambridge University Press, 2005), Chap. 5, pp. 166-227.

[10] B. M. Hochwald, T. L. Marzetta and V. Tarokh, "Multiple-antenna channel hardening and its implications for rate feedback and scheduling," *IEEE Trans. Inf. Theory* **50**, 1893-1909 (2004).

[11] M. Stojanovic, "Underwater acoustic communications," in *Encyclopedia of Electrical and Electronics Engineering* (John Wiley & Sons, 1999), vol. 22, pp. 688-698.

[12] Q. Ma and C. Tepedelenlioglu, "Practical multiuser diversity with outdated channel feedback," IEEE Trans. Veh. Technol. **54**, 1334-1345, 2005.